Journal of Geochemical Exploration 197 (2019) 238–250

Contents lists available at ScienceDirect

Journal of Geochemical Exploration

journal homepage: www.elsevier.com/locate/gexplo

W and Li-Cs-Ta geochemical signatures in I-type granites – A case study from the Vosges Mountains, NE France

Benedikt M. Steiner

Camborne School of Mines, University of Exeter, Penryn TR10 9FE, United Kingdom

ARTICLE INFO

Keywords:
Vosges
Variscan orogeny
Granite
Peraluminous
Lithium
Tungsten
Exploration targeting

ABSTRACT

In light of the recent 'lithium boom', a screening study for Sn-W and Li-Cs-Ta deposits was carried out and located an early 1980s Bureau de Recherches Géologiques et Minières (BRGM) geochemical survey with W anomalies of > 50 ppm in the Sainte-Marie-aux-Mines area, NE France. These anomalous areas, along with historic mining of polymetallic veins in the area, led to the present investigation of the regional potential for Variscan vein-hosted Sn-W-Li-Cs-Ta and Mesozoic-Cenozoic Cu-Pb-Zn-As-Ag-Ni veins in the central Vosges Mountains.

A total of 144 stream sediment samples were collected in the central Vosges Mountains covering an area of > 200 km^2. Multi-element pXRF and ICP-MS assays revealed previously undescribed W-Li-Cs-Ta geochemical anomalies related to major ENE-WSW trending fault zones and splay faults in the I-type Central Vosges Mg-K ('CVMg-K') granite. Field mapping evidence, previously published age data along with strong geochemical fractionation trends obtained from K/Rb, Zr/Hf and Nb/Ta ratios, imply that the CVMg-K granites were intruded by younger crustal melts derived from crustal anatexis of metasedimentary and metaigneous source rocks, that potentially exploited pre-existing fault control, and subsequently fractionated and enriched incompatible elements of economic interest.

This study demonstrates that Sn-W-Li-Cs-Ta geochemical anomalies can occur in I-type granites, if later orogenic processes leading to crustal anatexis resulted in the production of peraluminous melts, strong magmatic fractionation and emplacement of mineralization along regional fault zones. Therefore, the presence of I-type granites in Variscan and other geological terrains should encourage regional Sn-W-Li-Cs-Ta exploration.

1. Introduction

Considering the global drive for the exploration of 'critical' metals in the 2010s, such as Sn, W and Li-Cs-Ta (commonly referred to as 'LCT'), a review and investigation of historic mining districts seems timely (Graedel et al., 2014). In Europe, mineralization related to the Variscan Orogeny accounts for a considerable amount of structurally-controlled hydrothermal Sn-W deposits, in particular the Cornubian Orefield (Simons et al., 2017), the French Massif Central (Marignac and Cuney, 1999) and the Erzgebirge (Thomas and Tischendorf, 1987). Cornwall and the Erzgebirge have recently experienced a rise in exploration activities and geological investigations (Neßler et al., 2013). These metallogenic districts share the presence of a metasedimentary protolith coupled with an orogenic or mantle-derived heat source leading to the generation and mobilization of Sn, W and Li-Cs-Ta enriched melts (Romer and Kroner, 2015).

In this study the Vosges Mountains, located in NE France, have been recognized as an overlooked province prospective for Sn-W and Li-Cs-Ta deposits. A geochemical survey conducted by BRGM in 1983, available on InfoTerre (BRGM, 2018), identified W concentrations of > 50 ppm in I-type Central Vosges Mg-K ('CVMg-K') granites near Sainte-Marie-aux-Mines. This area, known for historic mining of vein-hosted Pb, Ag and Cu, has been extensively studied in terms of Variscan tectonics (Tabaud et al., 2015, 2014; Kratinová et al., 2007) and archaeological aspects of Medieval mining (Forel et al., 2010). However, it has received little attention with regards to the occurrence of 'critical' metals and its economic exploration potential. In particular, there is a notable absence of studies explaining the presence of Sn-W mineralization in this geological setting. This paper therefore fills the gap between previous research on regional tectonics and magmatism and missing aspects of economic geology. Using regional stream sediment geochemistry, this study aims to delineate the rather unusual occurrence of Sn, W and Li-Cs-Ta in I-type CVMg-K granites and relates the enrichment of these elements to crustal anatexis of metasedimentary and metaigneous source rocks during later stages of the Variscan Orogeny.

E-mail address: b.steiner@exeter.ac.uk.

https://doi.org/10.1016/j.gexplo.2018.12.009
Received 7 August 2018; Received in revised form 19 November 2018; Accepted 9 December 2018
Available online 12 December 2018
0375-6742/

2. Geology and mineralization assemblages in the Vosges Mountains

2.1. Regional geology

The Variscan Orogen has formed as a result of Palaeozoic contractional and extensional regimes during the mid-late Carboniferous (330–310 Ma, Schulmann et al., 2014). The lithotectonic domains of the Rhenohercynian, Saxothuringian and Moldanubian represent juxtaposition of autochthonous and allochthonous material which derived from different tectonic plates. The Vosges Mountains and Schwarzwald (Black Forest) form the Palaeozoic basement and are divided into the Saxothuringian domain to the north and the Moldanubian to the south with the boundary defined by the Lalaye-Lubine and Baden-Baden fault zones in the Vosges Mountains and Black Forest, respectively (Fig. 1a; Skrzypek et al., 2014; Tabaud et al., 2014).

The Vosges Mountains consist of three primary domains: the southern Palaeozoic basin, the central high grade gneissic and granulitic domain and the northern low-grade Palaeozoic sedimentary sequences (Kratinová et al., 2007). The northern-central Vosges Mountains around the Champ du Feu Massif host I- and S-type magmatic rocks and are affiliated with the subduction of the Rhenohercynian oceanic crust underneath the Saxothuringian continental crust (Edel et al., 2013). The Lalaye-Lubine dextral shear zone constitutes the northern part of the central high grade zone with calc-alkaline, I-type ‘actinolite granites’ (von Eller et al., 1975), renamed to ‘Central Vosges Mg-K granites’ (‘CVMg-K’, Tabaud et al., 2015, Lardeaux et al., 2014), present resulting from partial melting of mantle sources to the south. Recent studies provided a zircon U-Pb age of the CVMg-K granite near Sainte-Marie-aux-Mines of 337.2 ± 1.8 Ma (sample CN6; Tabaud et al., 2015). The Sainte-Marie-aux-Mines fault zone is orientated NE-SW and dissects the high-grade domain, whilst felsic granulites, amphibolites and pods of peridotites are present to the east (Kratinová et al., 2007). Mid-crustal paragneisses dominate the footwall of the high-grade unit and have been subsequently intruded by the Western Central Vosges Granite (W-CVG) dated at 321.6 ± 2.8 Ma (sample G-G4; Tabaud et al., 2015). South of Sainte-Marie-aux-Mines, the Bilstein, Brézouard and Thannenkirch (BBTC) granites form part of the W-CVG and are oriented in a WSW-ENE direction parallel to a network of local sinistral shear zones. The Thannenkirch granite is a medium-grained porphyritic biotite granite (monzogranite), whereas the Brézouard and Bilstein granites are two-mica leucogranites dated at 330–325 Ma using ^{39}Ar-^{40}Ar, K-Ar and U-Pb on zircon and monazite (Kratinová et al., 2007). Nédeltcheva et al. (2006) describe a transition from metaluminous I-type granites to peraluminous S-type granites in a southward direction indicating partial melting of crustal material and metasedimentary source rocks. Tabaud et al. (2015) established that this widespread mid-crustal anatexis event, leading to the intrusion of the muscovite-biotite W-CVG granite, occurred at 330–320 Ma, i.e. 10–15 Ma after the initial emplacement of the CVMg-K granites, which provided an in situ radiogenic heat source for the subsequent melting of source rocks, such as paragneisses, immature felsic-intermediate metaigneous rocks and CVMg-K granitic rocks.

2.2. Mineralization assemblages in the Sainte-Marie-aux-Mines and Val d'Argent area

Abundant metal occurrences in the form of Pb, Ag, Cu and Fe are widespread in the crystalline Vosges Mountains and form part of a polymetallic ore suite worked in the Vosges over the last millennium (Forel et al., 2010). Mining dates back to the 10th century in the Sainte-Marie-aux-Mines area (Fig. 1b) with a major focus on Ag extraction and processing during the 15th and 16th centuries (Mariet et al., 2016). This gave the valley its later name of ‘Val d'Argent’. The principal mining areas are subdivided into the Altenberg and Neuenberg zones with the Altenberg veins exploited until 1550, when work shifted to the Neuenberg zone (Mariet et al., 2016). Extraction of metals ceased in the mid 20th century due to a combination of resource depletion and mining finance.

Post-Variscan, low temperature polymetallic vein associations show remarkable similarities in both the Vosges Mountains and Schwarzwald and are related to Mesozoic and Cenozoic reactivation of Permian faults (Dekoninck et al., 2017). Within the Sainte-Marie-aux-Mines area different types of polymetallic veins are known. The Neuenberg veins strike E-W and carry Cu-Ag-As and Pb-Zn, whilst the Altenberg veins strike N-S and carry Pb-Zn-Ag. This is exemplified in the Gabe Gottes Mine where fault-controlled 20 to 500 mm wide veinlets contain sulphide-sulphosalt assemblages, including rare Pd tellurides, striking 80°–110° (Hafeznia et al., 2012). This mineralization style has similarities with other deposits in southwest Germany, particularly the Schwarzwald, where a major unconformity dividing the Permian (Zechstein) sedimentary rocks from the Variscan crystalline basement and a varied degree of mixing of Mesozoic of sedimentary brines with basement-derived fluids led to the emplacement of hydrothermal vein mineralization (Walter et al., 2017; Fusswinkel et al., 2014). The Wittichen deposit, for example, shows a sequence of three distinct base and precious metal mineralization events during the Permian-Miocene. Multi-stage Ag-Bi-Co-Ni-U and Cu-Bi veins occur within Variscan leucogranites and unconformably overlying Permo-Triassic red beds. F, Bi and to a minor extent REE are thought to originate from Variscan granitic sources whilst Ag-Co-Ni-Cu were leached from overlying red beds with an increasing influence of sedimentary brine and Permian red bed-derived fluids (Staude et al., 2012). Markl et al. (2016) postulated that the ‘five element vein-type’ assemblage (Ag-Co-Ni-Bi-As) found across the European Variscides formed in rapid, disequilibrium processes related to ‘natural fracking’. This process refers to the liberation of hydrocarbon-bearing fluids during fracturing of rocks and subsequent mixing with metal-rich hydrothermal fluids leading to ore precipitation.

In the Vosges Mountains, similar to the Cornubian Orefield and the Erzgebirge, lower Palaeozoic metasedimentary rocks were intruded by Carboniferous Variscan S-type granites leading to a number of syn- and post-magmatic mineralization assemblages. These peraluminous two-mica granites and to a lesser degree peripheral pre-Variscan metamorphic rocks are enriched in Sn, W, Mo, Cu, Fe, Mn and U (Dekoninck et al., 2017; Fluck and Weil, 1976). The metals are vein-hosted and often occur within structurally-controlled granitic cupolas comparable to the Massif Central (Cuney et al., 1990). In contrast to the known polymetallic suite, however, the occurrence of Sn-W-Li-Cs-Ta geochemical signatures has not been described in the study area.

3. Methodology

Stream sediments reflect the geology of upstream catchment areas and therefore can imply the presence of several lithological groupings in one sample (Hale and Plant, 1994). The measured chemical composition of stream sediments pertains to the catchment bedrock geology, overburden, and mineralization. 144 stream sediment samples have been collected from first and second order streams in the Sainte-Marie-aux-Mines-Lièpvre-Urbeis and Lubine area (Fig. 1b). The sample locations were designed to incorporate aspects of the BRGM regional geological map and prevailing catchment basins. Samples were collected from sediment traps, such as large boulders or point bars and sieved in the field to < 2 mm resulting in average weights of 500 g per sample. All samples were stored in plastic sample bags and labelled with sample ID, coordinates and elevation. The fine fraction size was allowed to settle in the bag before excess water was disposed back into the stream. The sampling equipment was thoroughly cleaned to prevent cross contamination.

Simultaneously, a comprehensive list of stream sample attribute data (colour, grain and mesh size, contamination etc.) was recorded on an iPad using the ‘Collector for ArcGIS’ app which facilitates data

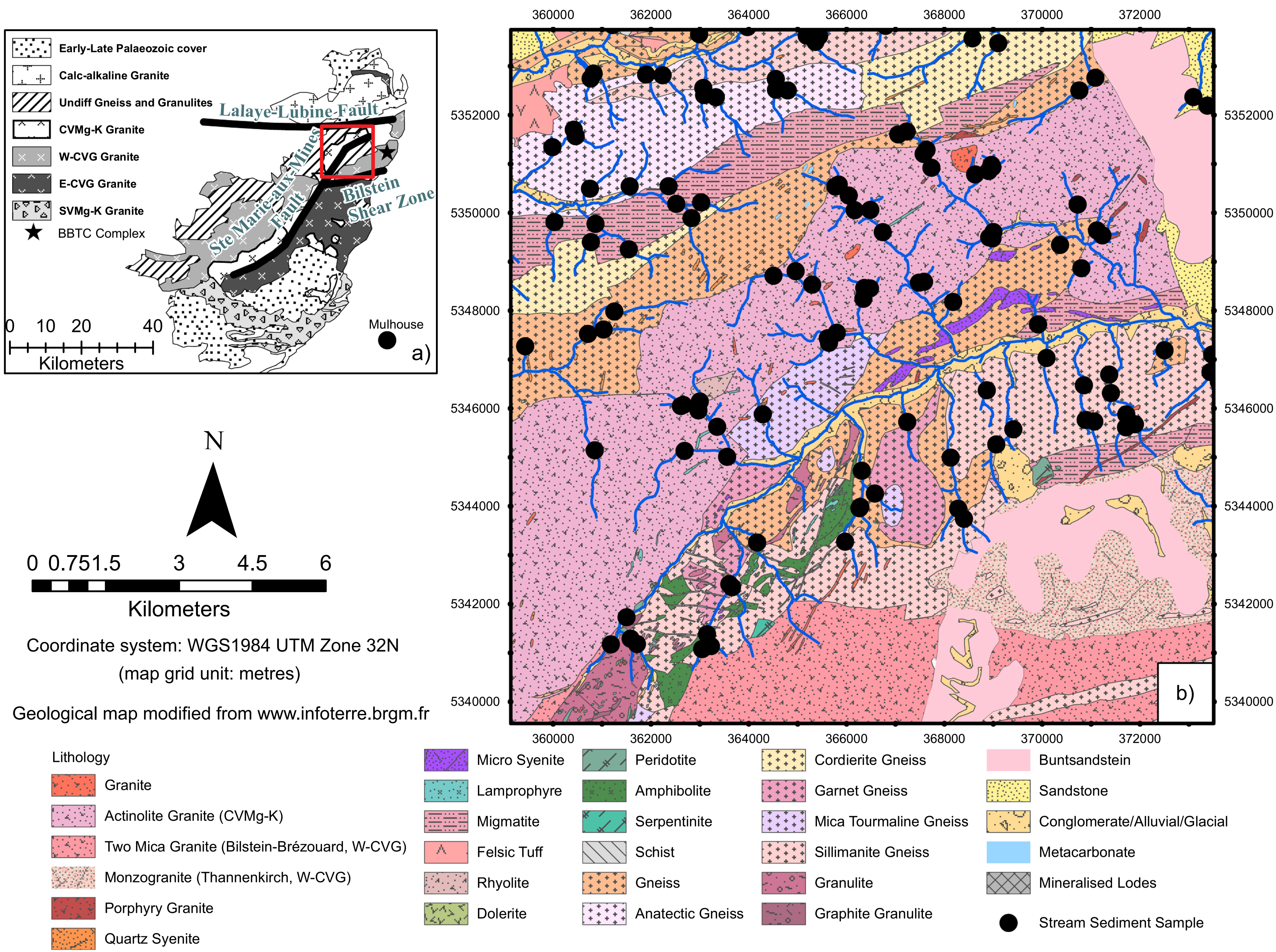

Fig. 1. a) Regional geological setting of the Vosges Mountains modified from Tabaud et al. (2015) and b) geological map of the Sainte-Marie-aux-Mines area, NE France, with stream sediment sample locations. (Modified from BRGM, 2018).

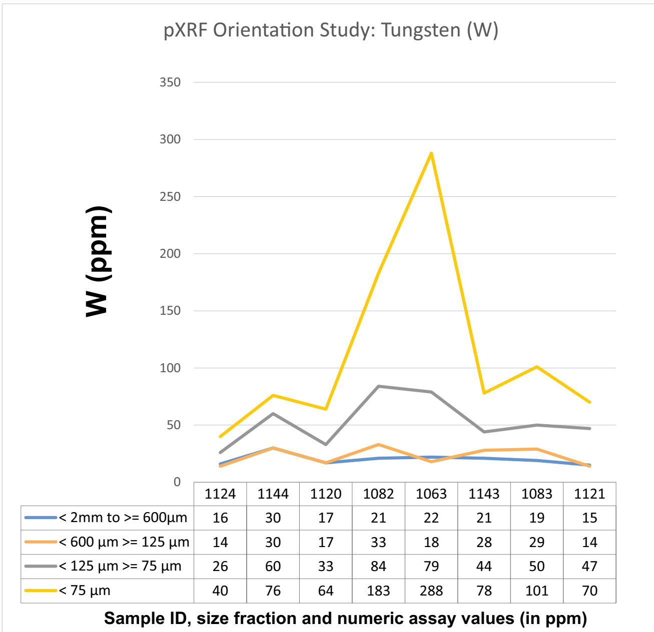

	1124	1144	1120	1082	1063	1143	1083	1121
< 2mm to >= 600µm	16	30	17	21	22	21	19	15
< 600 µm >= 125 µm	14	30	17	33	18	28	29	14
< 125 µm >= 75 µm	26	60	33	84	79	44	50	47
< 75 µm	40	76	64	183	288	78	101	70

Fig. 2. Results of an orientation study carried out using portable pXRF equipment in order to determine the most suitable grain size fraction for the present stream sediment sampling campaign.

management and integration with GIS software. Daily data checks, uploads and synchronisation ensured that the accumulating attribute data was free of errors. In addition, a visual inspection of stream sediment and larger boulders was recorded in order to aid the lithological classification of samples and the identification of fractionated lithologies, such as quartz or pegmatite-rich rock.

Samples were loaded into laboratory ovens in order to completely dry out at 40 °C. The samples were subsequently sieved through a Pascal Sieve Shaker passing 600 µm, 125 µm and 75 µm. Each sample was weighed before and after sieving to assess individual fraction weights and whether any sample loss had occurred.

An initial orientation study using a Olympus DP 6000 portable XRF (pXRF) determined the < 75 µm fraction to host the most pronounced anomalies for Sn, W and Cu (exemplified by the W plot in Fig. 2). This is in line with orientation studies discussed in Fletcher (1997) who recognized that fractions of heavy mineral associated elements finer than 100 µm are less influenced by local hydraulic effects and therefore represent the catchment area best and provide the most consistent anomalous dispersion trains. All 144 samples were subsequently analysed by pXRF in soil mode using the < 75 µm fraction. In addition to regular calibrations using Si quartz, three repeated measurements were taken and an average value calculated for each sample. 142 samples of the < 75 µm fraction were selected from the pXRF database for additional ICP-MS analysis using a standard Four Acid Digest and Agilent 7700 × ICP-MS instrument in order to obtain a wider range of trace and pathfinder elements at lower detection limits (Table 1).

Subsequent geochemical interpretations utilised pXRF assays for Sn and W and ICP-MS assays for all other trace elements following a workflow described in Steiner (2018). Initial classification of lithological units was achieved by delineating population clusters in bivariate geochemical plots, whereby each sample point was assigned a lithology, which was then refined using geological observations in upstream catchment areas and float to better represent subtle nuances in geochemical composition, for example 'CVMg-K Granite with abundant biotite and hornblende'.

4. Results

4.1. Polymetallic Cu, Co, Ni, Pb, Zn and Ag mineralization

Graduated point symbol maps of a series of base and precious metals commonly found in post-Variscan polymetallic vein assemblages (Cu, Co, Ni, Pb, Zn, and Ag; Markl et al., 2016) demonstrate enrichment in the gneissic country rock in the northern and southern part of the study area, Urbeis-Lubine and Tellure and Mines de Plomb, respectively (Fig. 3). At Tellure and Mines de Plomb, in particular, Ni was enriched by a factor of 3.75 compared to average crustal abundance values listed in Mazzucchelli (2011), Zn by a factor of 7.5, Pb by a factor of 69, and Ag by a factor of up to 7500. The presence of the polymetallic metal suite in the study area confirms and outlines, albeit at regional scale, previously described mineralization and historic mining locations. The focus of this study, however, will be on the presence of undescribed Sn-W-Li-Cs-Ta mineralization styles and lithogeochemical signatures of the principal mineralization host rocks.

4.2. Lithogeochemical classification of principal rock units and magmatic fractionation

Five main regional lithologies were distinguished in the dataset using characteristic trace element concentrations and assemblages supported by field observations in streams and outcrops, where possible (Figs. 4, 6–7; Table 2). These lithologies are regional in nature and represent a simplified snapshot of the BRGM map, aiding the determination of significant lithological compositions and petrogenetic processes, such as magmatic fractionation. Elements employed in this study to differentiate the geochemically differing suites of granites and metasedimentary rocks are principally immobile transition row and rare earth elements (REE), such as Sc, TiO_2, Th, Y and Zr.

'Undifferentiated gneissic and granulitic metasediments' plot as a distinctive population and are generally characterised by transition row and REE concentrations of Sc (9–35 ppm), Th (10–65 ppm), Ce (40–400 ppm) and Y (10–55 ppm). This population locally shows high concentrations of Cr (up to 350 ppm) and Nb (up to 45 ppm).

The 'CVMg-K Granite with abundant biotite and hornblende' was macroscopically distinguished from other felsic and metasedimentary rocks by a strong abundance of actinolite (40%), biotite (15%), feldspars (30%) and a lack of quartz (15%) (Fig. 5a). This population shows strong enrichment in Sc (10–150 ppm), TiO_2 (0.3–1 wt%), Th (70–345 ppm), Nb (15–70 ppm), Ce (150–2050 ppm), Y (50–390 ppm), Zr (600–7000 ppm) and a Th/U ratio < 4 (Fig. 4). Unusually high Sc, TiO_2, and Cr values characterize this felsic population compared to crustal and granitic abundance values (Mazzucchelli, 2011) implying the presence of Cr- and Ti-rich phases. The 'CVMg-K Granite with abundant biotite and hornblende' population plots along a distinctive SW-NE trend which resembles the strike of the 'actinolite granite' mapped by BRGM (Fig. 8). In addition, a number of samples plot in the metamorphic country rock in the Weissenbach and Lubine areas consistent with the proximity to the main granite body as well as previously mapped quartz syenite dykes and off-shoots into the country rock.

Concentration values for Sc (12–21 ppm), TiO_2 (0.4–0.6 wt%), Th (80–271 ppm), Ce (500–1600 ppm), Y (55–140 ppm) and 33 < Zr/Hf < 36 are considered typical for the 'Thannenkirch-Brézouard-Bilstein Granite' located in the southern part of the study area. On the BRGM map, this geochemical population plots in a sillimanite gneiss

Table 1
Summary statistics of key elements used in the present geochemical study. Sn and W were analysed by pXRF (144 samples), all other trace elements by ICP-MS using a four acid digest (142 samples). The stream sediment grain size fraction analysed throughout the study was < 75 µm.

	Ag (ppm)	Ce (ppm)	Co (ppm)	Cr (ppm)	Cs (ppm)	Cu (ppm)	Hf (ppm)	K_2O (wt %)	Li (ppm)	Nb (ppm)	Ni (ppm)
Lower limit of detection	0.0003	0.0003	0.0006	0.0003	0.0007	0.00005	0.0003	0.09	0.0002	0.0003	0.0003
Minimum	< 0.0003	43.4	1.35	20.73	6.28	10.22	3.24	0.8	12.98	4.47	6.94
Maximum	524.12	2039.14	29.27	348.7	75.01	305.75	805.86	3.7	830.2	121.5	297.41
Mean	4.65	361.84	11.79	128.32	29.13	52.53	59.62	2.17	76.54	24.58	46.47
Median	0.0003	249.45	11.51	94.48	25.99	43.33	18.28	2.1	65.22	17.95	41.98
5th percentile	< 0.0003	98.76	5.64	47.64	10.74	18.33	4.3	1.4	27.06	11.24	19.85
10th percentile	< 0.0003	113.67	6.32	58.49	14.16	20.92	5.37	1.5	35.87	12.41	22.69
25th percentile	< 0.0003	175.8	8.63	73.21	19.57	30.3	8.94	1.88	48.94	14.23	30.92
30 percentile	< 0.0003	187.07	9.26	78.57	20.65	32.01	9.81	1.9	53.1	14.77	33.96
60th percentile	0.1	315.75	12.11	119.74	29.84	49.43	27.06	2.2	69.8	21.01	44.9
75th percentile	0.28	475.5	14.36	176.04	37.71	57.97	77.2	2.53	87.45	32.09	53.91
80th percentile	0.42	522.56	15.05	201.07	40.12	63.12	110.61	2.6	93.53	38.35	61.74
90th percentile	0.9	755.12	16.7	246.83	46.86	83.39	149.9	2.8	114.2	43.67	69.79
95th percentile	1.5	875.64	19.78	299.51	55.56	115.5	189.7	3	143.78	51.2	77.43
98th percentile	24.68	1265.24	28.02	317.88	64.99	210.08	462.5	3.31	215.08	73.06	115.23
99th percentile	348.99	1895.74	28.82	343.88	71.47	278.29	701.43	3.57	612.42	107.51	238.35

	Pb (ppm)	Rb (ppm)	Sc (ppm)	Sn (ppm)	Ta (ppm)	Th (ppm)	TiO_2 (wt %)	W (ppm)	Y (ppm)	Zn (ppm)	Zr (ppm)
Lower limit of detection	0.0003	0.0003	0.0003	6.7	0.0003	0.0003	0.0007	3.5	0.0002	0.0002	0.0003
Minimum	16.63	50.8	5.67	< 6.7	0.43	9.74	0.22	< 3.5	11.55	28.3	119.26
Maximum	962.22	589	324.82	36	28.9	587.33	1.02	578	384.42	565.76	35,987.-15
Mean	53.55	160.14	29.89	8.03	3.29	92.31	0.54	87.8	59.48	133.03	2218.23
Median	35.05	141.2	17.12	< 6.7	2.5	78.2	0.51	70.5	49	112.26	670.74
5th percentile	18.28	70	9.3	< 6.7	1.09	15.29	0.35	21.1	15.81	51.94	162.57
10th percentile	20.57	89.56	9.87	< 6.7	1.28	17.61	0.38	32.3	22.56	59.04	201.15
25th percentile	27.96	113.34	12.12	< 6.7	1.62	41.37	0.42	48	35.06	79.78	335.69
30 percentile	29.28	119.75	13.05	< 6.7	1.69	46.18	0.44	51.9	38.58	83.89	363.29
60th percentile	37.38	161.76	21.6	< 6.7	3.04	92.56	0.54	76	55.95	131	1020.48
75th percentile	43.29	201.66	38.3	< 6.7	3.92	124.35	0.64	106.25	71.03	149.13	2934
80th percentile	46.94	211.42	46.25	< 6.7	4.65	129.55	0.68	124.4	77.71	164.23	3988.04
90th percentile	73.93	248.61	61.31	< 6.7	5.56	159	0.75	172.4	93.64	209.33	5461.2
95th percentile	99.8	275.92	70.92	22	7.32	218.84	0.85	218.05	114.62	315.1	6659.02
98th percentile	335.15	310.75	155.65	28.7	13.54	396.28	0.97	250.04	256.94	451.86	16,331.-52
99th percentile	784.16	491.01	267.71	34.71	26	564.91	1.01	450.29	381.59	558.9	29,667.-78

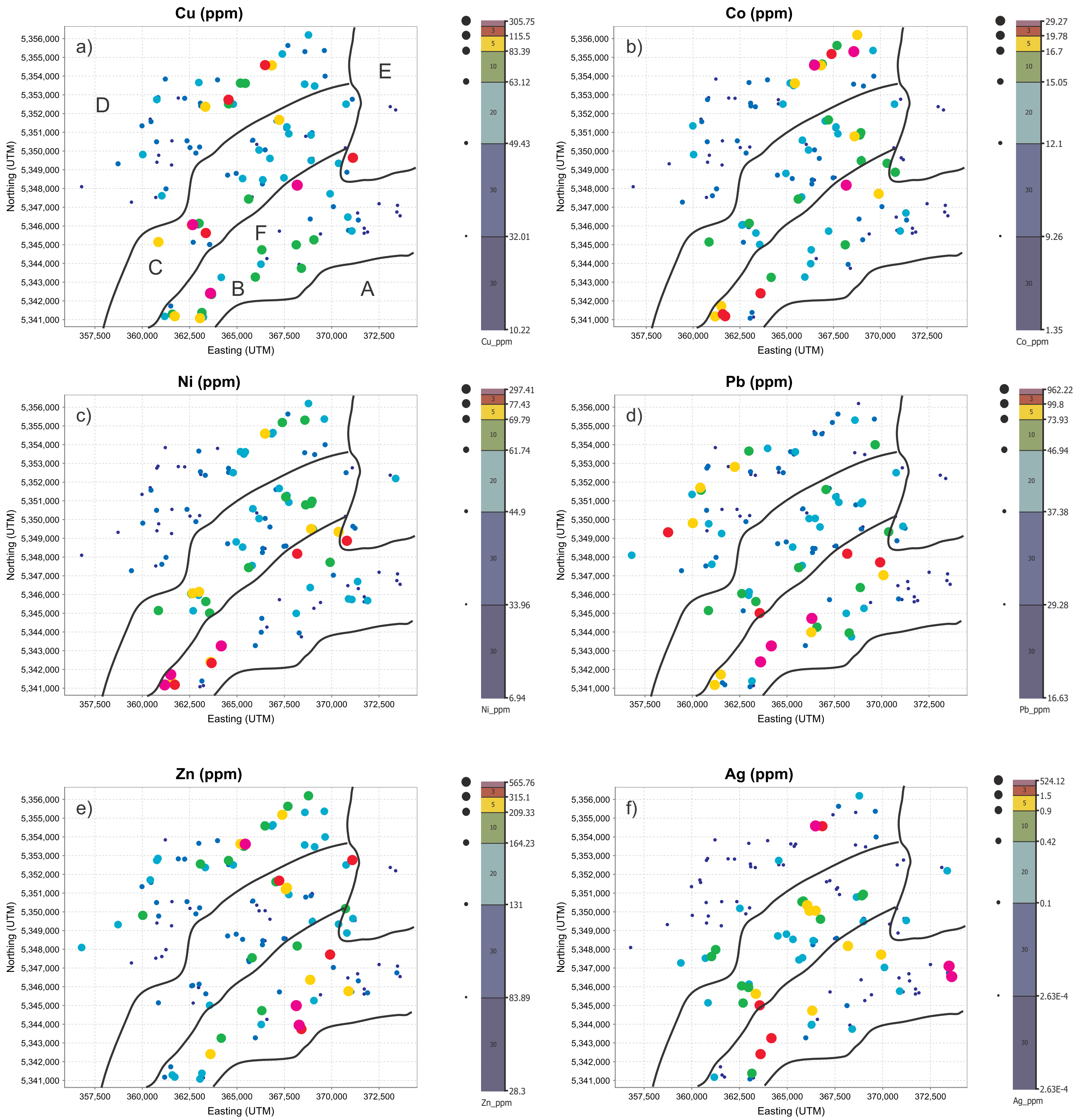

Fig. 3. Graduated point symbol maps for a) Cu, b) Co, c) Ni, d) Pb, e) Zn and f) Ag using 30th, 60th, 80, 90th, 95th and 98th percentile distribution from Table 1. Principal geological domains are highlighted in panels a–f with abbreviations provided in panel a: A – Thannenkirch-Bilstein-Brézouard Granite, B – Gneisses and Granulites of the Val d'Argent, B is also the location of the Tellure and Mines de Plomb mineral occurrences, C – CVMg-K granite, D – Gneisses and Migmatites of the Liepvre-Urbeis Valleys, E – Mesozoic Buntsandstein cover, F – Location of Sainte Marie-aux-Mines. The post-Variscan poly-metallic association is associated with domains B and D.

unit, however, less than one kilometre downstream from known Thannenkirch and Brézouard-Bilstein granite occurrences. High concentrations of immobile elements and REE, particularly Ce, indicate a distinctive felsic geochemical signature of these stream sediment samples.

'Migmatite-Granites' generally have lower Th (65–125 ppm), Ce (430–860 ppm) and TiO_2 (0.4–0.5 wt%) abundances than the Thannenkirch-Bilstein Granite and are characterised by a Zr/Hf ratio between 37 and 42. The population is predominantly present in the northern part of the study area between Urbeis and Provenchères-sur-

Fig. 4. Mapping of litho-geochemical populations using binary plots of Sc vs a) Th, b) TiO_2, Nb, d) Ce, e) Y and f) Cr. The CVMg-K granite is characterised by anomalous abundances of Th, Sc, Nb, Ce, Cr and Y.

Table 2
Lithological classification of geochemical populations in the Sainte Marie-aux-Mines stream sediment geochemistry dataset. The range of characteristic major and trace element concentrations is provided for each population along with a summary of the relation between mapped populations and the BRGM geological map.

Lithological classification	Geochemical plot	Elemental signature	Relation to BRGM map
Undifferentiated gneissic and granulitic metasediments	Sc vs Th, Ce, Y, Cr, Nb	Sc (9–35 ppm), Th (10–65 ppm), Ce (40–400 ppm) and Y (10–55 ppm). Locally, Cr (up to 350 ppm) and Nb (up to 45 ppm).	Trace previously mapped high grade gneisses and granulites south and north of Sainte Marie-aux-Mines
CVMg-K Granite with abundant biotite and hornblende	Sc vs TiO_2, Th, Nb, Ce, Y, Cr	Sc (10–150 ppm), TiO_2 (0.3–1 wt%), Th (70–345 ppm), Nb (15–70 ppm), Ce (150–2050 ppm), Y (50–390 ppm), Zr (600–7000 ppm)	Plots along a distinctive SW-NE trend which resembles the strike of the 'actinolite granite' mapped by BRGM
Thannenkirch-Brézouard-Bilstein Granite	Sc vs Th, Nb, Ce, Y, Cr, Zr/Hf	Sc (12–21 ppm), TiO_2 (0.4–0.6 wt%), Th (80–271 ppm), Ce (500–1600 ppm), Y (55–140 ppm) and 33 < Zr/Hf < 36	Population plots in a sillimanite gneiss unit, however, less than one kilometre downstream from known Thannenkirch and Brézouard-Bilstein granite occurrences.
Migmatite-Granites	Sc vs TiO_2, Th, Ce, Zr/Hf	Th (65–125 ppm), Ce (430–860 ppm) and TiO_2 (0.4–0.5 wt%). 37 < Zr/Hf < 42	Located in the northern part of the study area between Urbeis and Provenchères-sur-Fave.
Hydrothermally-altered granite with W-Li-Cs-Ta signature	Nb/Ta vs K/Rb and Zr/Hf and K/Rb vs Li, Cs, Ta, W	Nb/Ta < 5 and 36 < Zr/Hf < 39, Li (50–830 ppm), Cs (8–58 ppm), Ta (8–28 ppm), W (50–250 ppm)	Strongly associated with *E*-W to SW-NE trending faults in the CVMg-K granite constituting the prevailing network of first and second order streams in the study area.

Fave.

In order to determine distinctive fractionation trends in granitic subpopulations, further fractionation indices discussed by Ballouard et al. (2016) were applied to the dataset: characteristic K/Rb ratios < 150 indicate pegmatite-hydrothermal evolution along with increased fractionation and enrichment of W, Li, Cs and Ta (Fig. 6). The degree of fractionation was defined by assessing clustering of all previously determined felsic populations with decreasing K/Rb values: weakly (K/Rb > 120) and moderately-strongly (K/Rb < 120) fractionated. The application of additional petrogenetic markers, such as K/Rb vs Zr/Hf and Nb/Ta vs Zr/Hf, aim to further distinguish highly fractionated granites with a distinct influence of magmatic-hydrothermal interaction during fractional crystallisation (Fig. 7; Bau, 1996; Linnen and Keppler, 1997). Samples with Nb/Ta < 5 and 36 < Zr/Hf < 39 were classified as 'hydrothermally-altered granite with W-Li-Cs-Ta signature' in line with other comparative studies carried out by Ballouard et al. (2016). This population predominantly plots in or in close vicinity to the 'CVMg-K granite with abundant biotite and hornblende' outlined in this study and by Tabaud et al. (2015). It is furthermore strongly associated with *E*-W to SW-NE trending faults constituting the prevailing network of first and second order streams in the study area, and supported by grab samples of leucogranitic, pegmatitic, feldspar-rich rock with minor muscovite, biotite and quartz collected in the otherwise ubiquitous 'CVMg-K granite with abundant biotite and hornblende' northeast of Wisembach and Baligoutte (Fig. 5b, c and indicated on map Fig. 8).

5. Discussion

The graduated point symbol maps demonstrate a pronounced enrichment of Cu, Co, Ni, Pb, Zn and Ag in metasedimentary country rock, particularly in the Val d'Argent and Urbeis valleys (Fig. 3).

These rocks contain a comparably lower, but still remarkably high, content of immobile trace elements indicating a distinctive felsic signature in the catchment areas. The 'CVMg-K granite with abundant biotite and hornblende has a remarkably high concentration of Sc, TiO_2, Zr, Cr and Nb (Fig. 4) and contains pronounced anomalies of Sn, W, Li, Cs, Ta (Fig. 6). Elevated Sc is interpreted to result from the substitution of Fe^{3+} with Sc^{3+} in mafic minerals, such as amphibole, biotite and pyroxene (Norman and Haskin, 1968), commonly present in I-type granites, and mafic restites that were observed in calc-alkaline, mantle-sourced magmas of the Central and Northern Vosges (Tabaud et al., 2015; von Eller et al., 1975). The high Cr, TiO_2 and Zr concentration in the stream sediment samples is, in particular, most likely a result of the accumulation of heavy minerals in stream trap sites. Sphene, monazite and zircon were described in the CVMg-K granite (Tabaud et al., 2015; von Eller et al., 1975) adding to the high Cr, TiO_2 and Zr, respectively. This is supported by one sample of 36,000 ppm Zr (Table 1) implying a very high abundance of heavy accessory minerals in the sample.

I-type granites enriched in incompatible and high field strength elements have been described in the Mount Pleasant area, New Brunswick, and were related to partial melting and strong fractionation of crustal quartzofeldspathic sources under relatively low temperatures (Yang et al., 2008). Romer and Kroner (2015), on the other hand, emphasise the importance of i) intensely chemically weathered, and therefore Li, Cs, Sn, and W-enriched sedimentary protolith, ii) accumulating along continental margins, and iii) the presence of an orogenic and mantle-derived heat source during subduction and melting processes resulting in the preferential formation of Sn, W and Li-Cs-Ta mineralization astride major suture zones. The Vosges Mountains, along with other European Variscan orogens, are considered to be representative of this tectonic and geological setting. With increasing fractionation and contribution of late-stage magmatic processes, peraluminous granitic and pegmatitic melts are enriched in B, F, P acting as fluxing elements that lower the melting temperature and allow incompatible and high field strength elements, such as Sn, W, Nb and Ta to be retained in low temperature melts (Gao et al., 2016; Ballouard et al., 2016; Linnen et al., 2012; Zaraisky et al., 2010). When the fluxing elements are removed during crystallisation of tourmaline or fluorite, for example, Nb, Ta and W partition into silicates and oxides as demonstrated in the Cornubian Batholith (Simons et al., 2017) or the Massif Central (Cuney et al., 1990).

The enrichment of incompatible elements during magmatic fractionation can be explained by changes of elemental ratios in K/Rb vs Nb/Ta and Zr/Hf bivariate plots (Ballouard et al., 2016). K/Rb values < 150 indicate a transition to pegmatite-hydrothermal evolution of the granitic melt due to the preferential substitution of K with Rb in micas and feldspars (Shaw, 1968). Nb/Ta values < 5 imply an increase in secondary muscovitisation and hydrothermal sub-solidus reactions leading to preferential fractionation of Nb over Ta, whereas the Zr/Hf

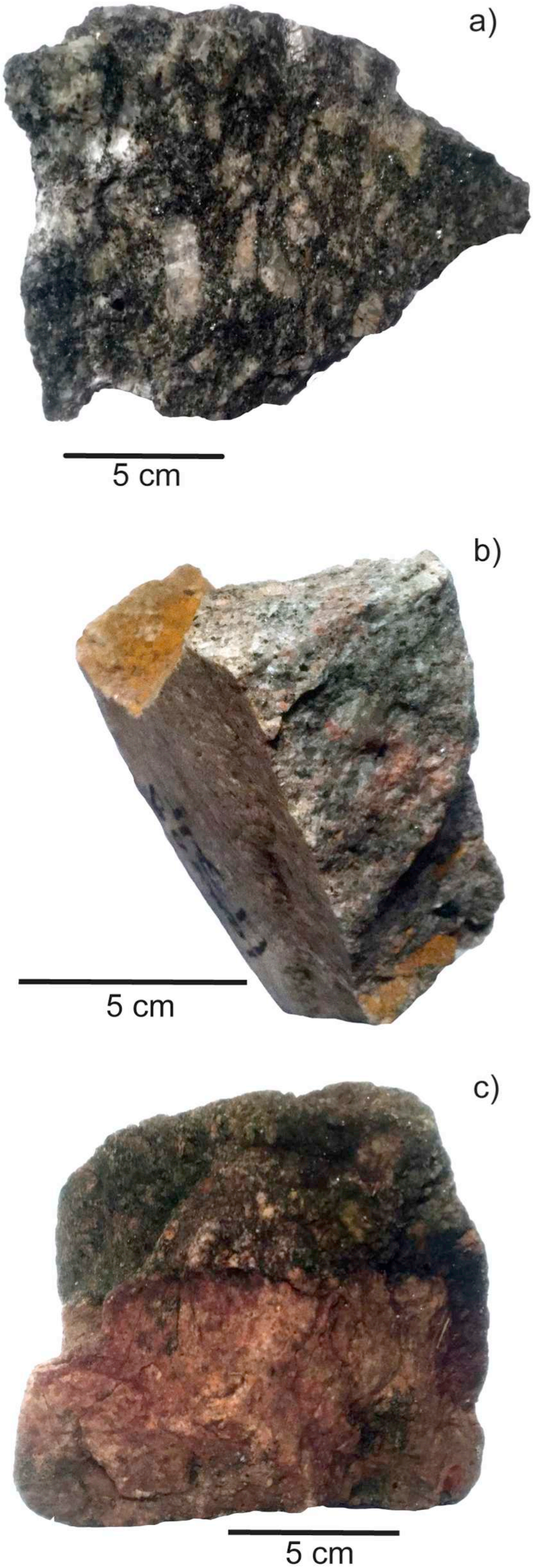

Fig. 5. Typical rock specimens of a) 'CVMg-K granite with abundant biotite and hornblende', b) leucogranite with minor muscovite and biotite and c) pegmatitic vein in CVMg-K granite with abundant K-feldspar and quartz. 5b and c have been encountered in fault-controlled streams and gorges in the Wisembach and Baligoutte areas.

ratio describe the fertility of evolving melts as Kd values of Hf in zircon increase with magmatic fractionation (Bau, 1996; Fujimaki, 1986). Considering the nature of the sampled stream sediment, secondary dispersion processes will lead to partial dissolution of mineral phases, enrichment of heavy accessory minerals and changes in elemental abundances (Guagliardi et al., 2013; Fletcher, 1997; Hale and Plant, 1994). For example, it cannot be entirely ruled out that due to the higher density of micas over feldspars and the preferred substitution of Rb for K in micas, relative enrichment of micas in stream sediment samples can result in decreasing K/Rb values, whereas Zr/Hf and Nb/Ta values in resistant minerals, such as zircon and columbite-tantalite, remain the same during sedimentation. In addition, stream sediments in fractionated and mineralised S-type granites typically show K/Rb values of 60–130 (Steiner, 2018) compared to lower values of 20–50 in outcrop and rock samples (Simons et al., 2017). Nevertheless, these three ratios provide a useful indicator for magmatic-hydrothermal interaction, the fertility of granitic rocks and therefore economic Sn-W-Li-Cs-Ta mineralization in late stage fractionated melts. In particular, the ratios delineate the unusual enrichment of W-Li-Cs-Ta in I-type CVMg-K granites in the study area. In Figs. 6 and 7 'hydrothermally-altered granite with W-Li-Cs-Ta signature' shows a distinctive correlation of W-Li-Cs-Ta enrichment with decreasing K/Rb and Nb/Ta values below 150 and 5, respectively. Weakly-moderately fractionated granite populations generally contain less concentrated Sn, W and Li-Cs-Ta than moderately and strongly fractionated granites. The anomalous samples are located along the prominent NE-SW trending Sainte-Marie-aux-Mines fault zone and splays separating the 'CVMg-K granite with abundant biotite and hornblende' in the northwest from 'undifferentiated gneissic and granulitic metasediments' in the southeast (Fig. 8). A strong structural control of W-Li-Cs-Ta mineralization within the CVMg-K granite is therefore evident. The occurrence of coarse-grained leucogranitic rocks along narrow SW-NE trending streams and fault zones (Fig. 5b, c) strongly indicates that, locally, magmatic fractionation processes led to the depletion of mafic and enrichment of felsic minerals. This further supports previously established geochemical indicators of locally strong magmatic fractionation in the 'CVMg-K granite with abundant biotite and hornblende'. Furthermore, this implies that highly fractionated and W-Li-Cs-Ta enriched melts are likely sourced from a postulated deep-seated, blind S-type granite body and moved upward emplacing mineralization in structural traps along the fault zone. The assumption is considered plausible as the original CVMg-K granite emplacement, dated at 337.2 ± 1.8 Ma, was followed by wide-spread mid-crustal anatexis of paragneisses, immature felsic-intermediate metaigneous rocks and CVMg-K granitic rocks leading to the emplacement of voluminous muscovite-biotite granite intrusions of the W-CVG at 330–320 Ma < 7 km further south (Tabaud et al., 2015). A close spatial co-existence of metasedimentary country rocks, younger S-type W-CVG and older I-type CVMg-K granites in the study area coupled with a previously established crustal anatexis event may therefore suggest a to date unknown S-type granite source in the CVMg-K granite.

6. Conclusions and implications for mineral exploration

The present study confirmed the occurrence of a polymetallic Cu, Co, Ni, Pb, Zn and Ag mineralization assemblage near Tellure and Mines de Plomb in the south, and Urbeis-Lubine in the north of the study area. The focus, however, was the delineation and interpretation of a rather unusual W-Li-Cs-Ta geochemical association found in I-type CVMg-K granites near Sainte-Marie-aux-Mines. Field observations and geochemical fractionation trends demonstrated that this particular

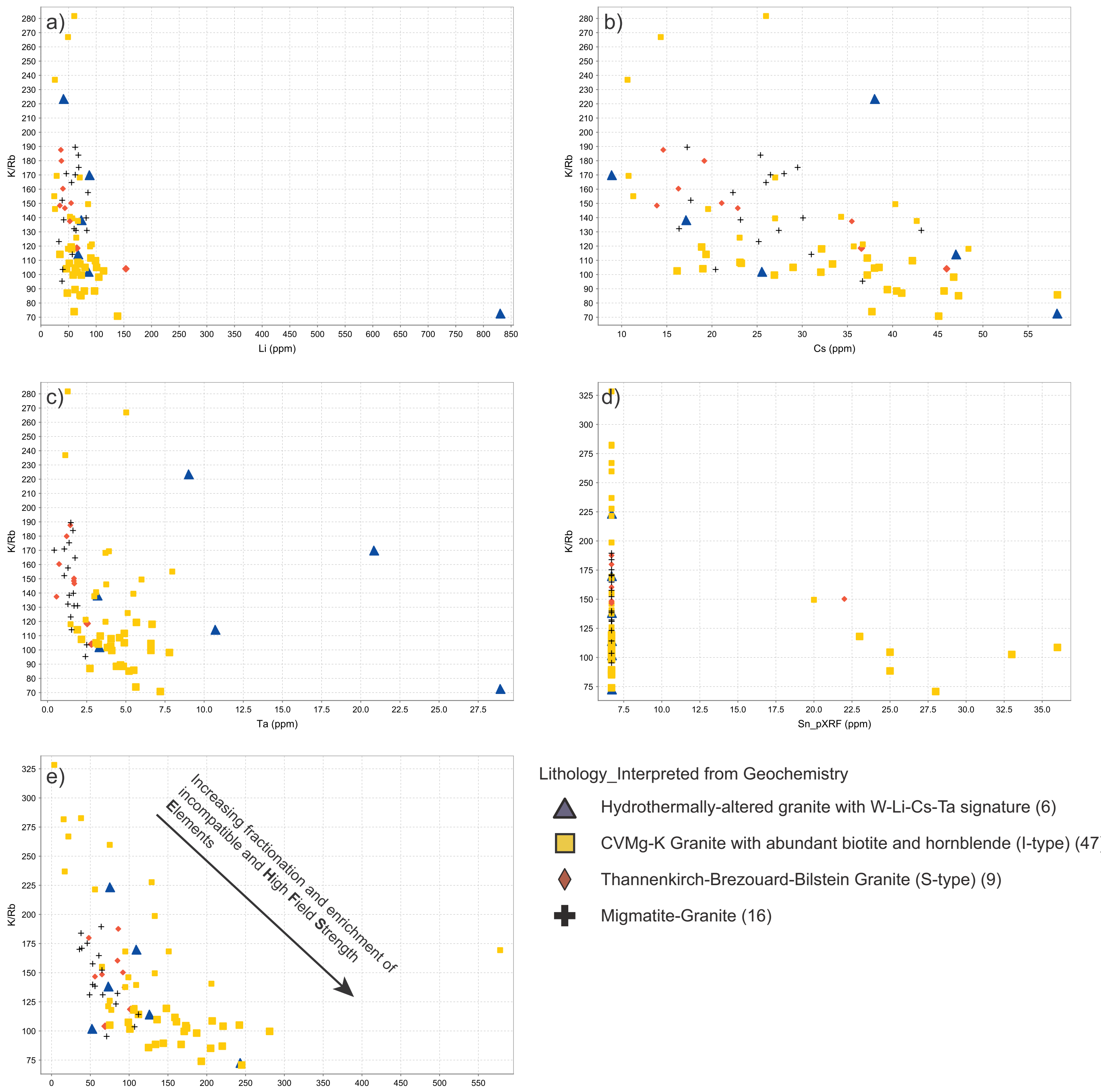

Fig. 6. Fractionation index K/Rb plotted against incompatible elements in Sn-W and Li-Cs-Ta suite. Three granite populations were determined by assessing clustering with decreasing K/Rb values: weakly and medium-strongly fractionated. Symbology as in Fig. 4.

element association is likely to be the result of a previously postulated wide-spread crustal anatexis at ca. 330–320 Ma, fuelled by in-situ radiogenic heat production of mid-crustal Mg-K granites (Tabaud et al., 2015). As a result, exploration for Sn-W and Li-Cs-Ta deposits in Variscan and other geological terrains should not strictly be limited to the surficial expression of large S-type granite bodies. Instead, Sn-W and Li-Cs-Ta geochemical anomalies can also be present in I-type granites, if later orogenic processes leading to crustal anatexis resulted in the production of peraluminous melts, strong magmatic fractionation and emplacement of mineralization along a regional network of fault zones. This to date unrecognized mineralization style in the Sainte-Marie-aux-Mines area will benefit from further genetic and economic investigations.

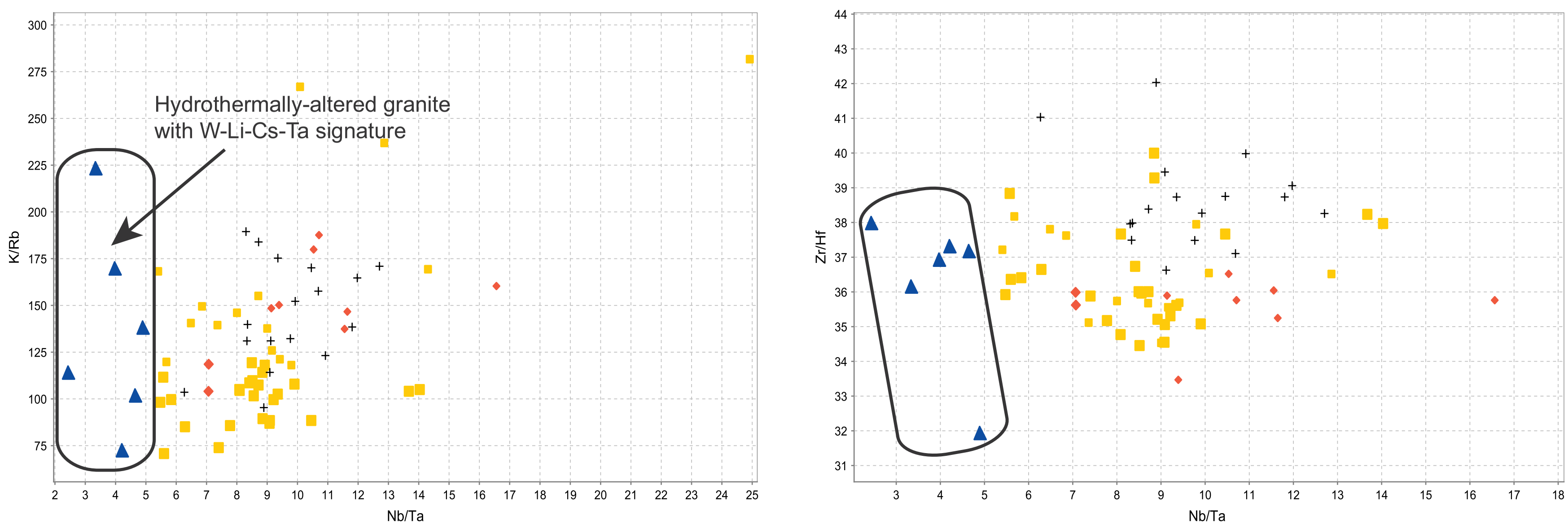

Fig. 7. Additional fractionation indices of Nb/Ta vs a) K/Rb and b) Zr/Hf allow to further distinguish highly fractionated granites with a distinct influence of magmatic-hydrothermal interactions during fractional crystallisation (Ballouard et al., 2016; Linnen and Keppler, 1997; Bau, 1996). Samples with Nb/Ta < 5 and Zr/Hf 32–39 were classified as 'hydrothermally altered granite with W-Li-Cs-Ta signature'. Symbology as in Fig. 4.

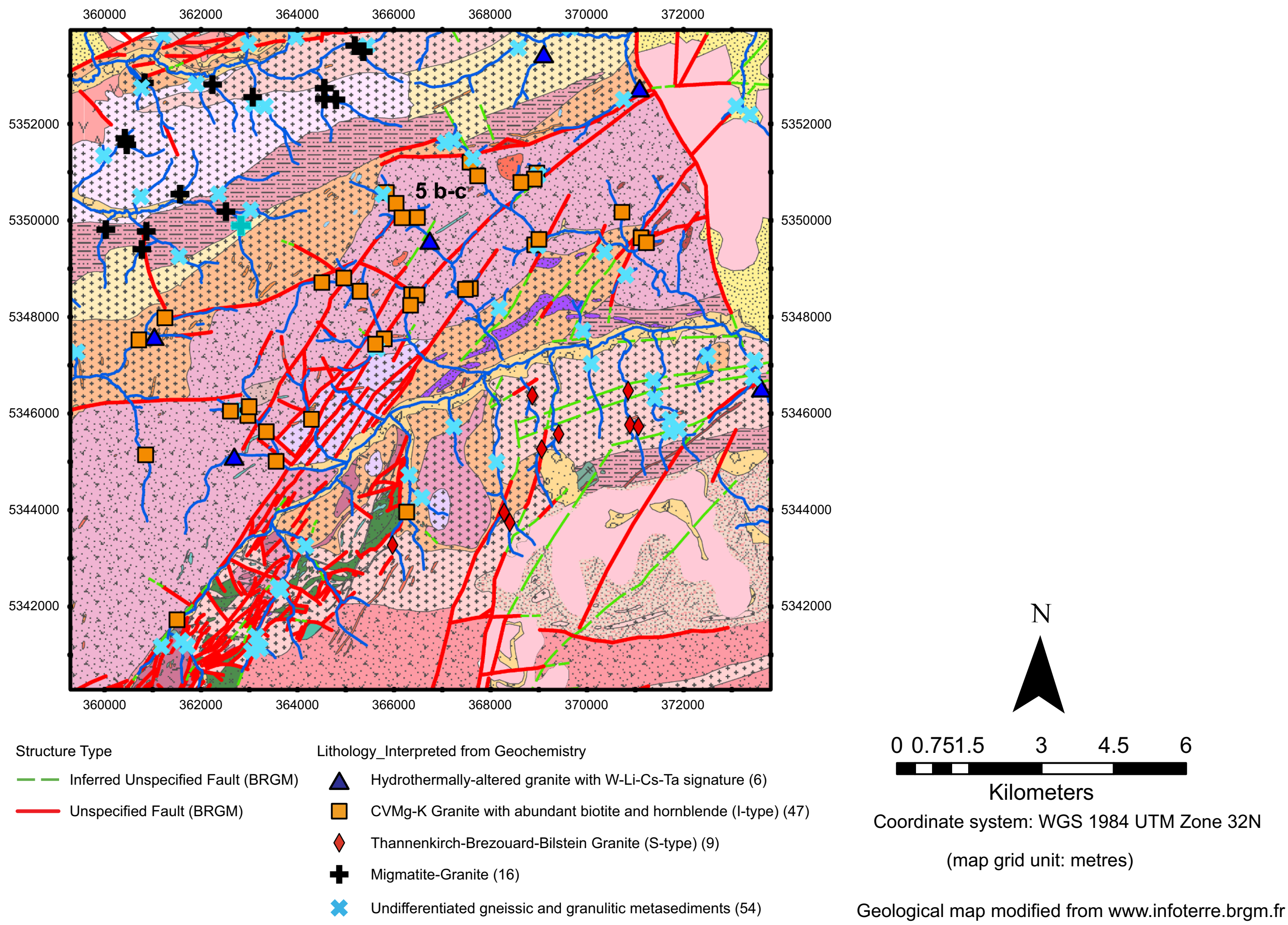

Fig. 8. Lithologies interpreted from stream sediment geochemistry on modified BRGM geological map and structures. The illustrated area covers the CVMg-K granite, northern part of the BBTC Complex and surrounding metamorphic rocks. Observed leucogranitic and pegmatitic rocks (location indicated as 5 b–c) along with interpreted 'hydrothermally-altered granites with W-Li-Cs-Ta signature' are principally located along SW-NE orientated fault systems in the CVMg-K granite. For explanation of rock types see Fig. 1b.

Acknowledgements

The author would like to thank Robin Shail, Jens Andersen and Hannah Hughes who critically commented on a first draft of the manuscript. Robert Ayuso, Karel Breiter and an anonymous reviewer are thanked for providing input during the revision process. Gavyn Rollinson and Sharon Uren at Camborne School of Mines are thanked for providing assistance with the analytical work. The author also thanks Nicholas Finlayson and James Barnet for help with sampling.

References

Ballouard, C., Poujol, M., Boulvais, P., Branquet, Y., Tartèse, R., Vigneresse, J.L., 2016. Nb-Ta fractionation in peraluminous granites: a marker of the magmatic-hydrothermal transition. Geology 44 (3), 231–234.
Bau, M., 1996. Controls on the fractionation of isovalent trace elements in magmatic and aqueous systems: evidence from Y/Ho, Zr/Hf, and lanthanide tetrad effect. Contrib. Mineral. Petrol. 123 (3), 323–333.
BRGM, 2018. BRGM InfoTerre [online]. Available from: http://www.infoterre.brgm.fr, Accessed date: 29 July 2018.
Cuney, M., Friedrich, M., Blumenfeld, P., Bourguignon, A., Boiron, M.C., Vigneresse, J.L., Poty, B., 1990. Metallogenesis in the French part of the Variscan orogen. Part I: U preconcentrations in pre-Variscan and Variscan formations—a comparison with Sn, W and Au. Tectonophysics 177 (1–3), 39–57.
Dekoninck, A., Rochez, G., Yans, J., Fluck, P., 2017. Mineralizing events in the Vosges massif: insights from the Mn-W Haut-Poirot deposit (NE France). In: Mineral Resources to Discover - 14th SGA Biennial Meeting. 4. pp. 1519–1522.
Edel, J.B., Schulmann, K., Skrzypek, E., Cocherie, A., 2013. Tectonic evolution of the European Variscan belt constrained by palaeomagnetic, structural and anisotropy of magnetic susceptibility data from the Northern Vosges magmatic arc (eastern France). J. Geol. Soc. 170 (5), 2011–2138.
Fletcher, W.K., 1997. Stream sediment geochemistry in today's exploration world. In: Gubins, A.G. (Ed.), Proceedings of Exploration '97: Fourth Decennial International Conference on Mineral Exploration.
Fluck, P., Weil, R., 1976. Géologie des gîtes minéraux des Vosges et des régions limitrophes. In: Corrélation métallogénique Vosges - Forêt-Noire. Mémoires du B.R.G.M.
Forel, B., Monna, F., Petit, C., Bruguier, O., Losno, R., Fluck, P., Begeot, C., Richard, H., Bichet, V., Chateau, C., 2010. Historical mining and smelting in the Vosges Mountains (France) recorded in two ombrotrophic peat bogs. J. Geochem. Explor. 107 (1), 9–20.
Fujimaki, H., 1986. Partition-coefficients of Hf, Zr, and REE between zircon, apatite and liquid. Contrib. Mineral. Petrol. 94 (1), 42–45.
Fusswinkel, T., Wagner, T., Wenzel, T., Wälle, M., Lorenz, J., 2014. Red bed and basement sourced fluids recorded in hydrothermal Mn–Fe–As veins, Sailauf (Germany): a LA-ICPMS fluid inclusion study. Chem. Geol. 363, 22–39.
Gao, P., Zheng, Y.F., Zhao, Z.F., 2016. Distinction between S-type and peraluminous I-type granites: zircon versus whole-rock geochemistry. Lithos 258, 77–91.
Graedel, T.E., Gunn, G., Espinoza, L.T., 2014. Metal resources, use and criticality. In: Gunn, G. (Ed.), Critical Metals Handbook. American Geophysical Union, Hoboken, NJ, pp. 1–19.
Guagliardi, I., Apollaro, C., Scarciglia, F., De Rosa, R., 2013. Influence of particle-size on geochemical distribution of stream sediments in the Lese river catchment, southern Italy. Biotechnol. Agron. Soc. Environ. 17 (1), 43–55.
Hafeznia, Y., Bourlange, S., Ohnenstetter, M., 2012. Tectonic conditions of hydrothermal polymetallic vein-type mineralization, Sainte Marie-aux-Mines, France. In: EGU General Assembly Conference Abstracts. 14. pp. 10–17.
Drainage geochemistry. In: Hale, M., Plant, J.A. (Eds.), Handbook of Exploration Geochemistry. vol. 6 Elsevier.
Kratinová, Z., Schulmann, K., Edel, J.B., Ježek, J., Schaltegger, U., 2007. Model of successive granite sheet emplacement in transtensional setting: integrated microstructural and anisotropy of magnetic susceptibility study. Tectonics 26 (6), 1–7.
Lardeaux, J.M., Schulmann, K., Faure, M., Janoušek, V., Lexa, O., Skrzypek, E., Edel, J.B.,

Štípská, P., 2014. The Moldanubian zone in the French Massif Central, Vosges/Schwarzwald and Bohemian Massif revisited: differences and similarities. Geol. Soc. Lond. Spec. Publ. 405, 7–44.
Linnen, R.L., Keppler, H., 1997. Columbite solubility in granitic melts: consequences for the enrichment and fractionation of Nb and Ta in the Earth's crust. Contrib. Mineral. Petrol. 128, 213–227.
Linnen, R.L., Van Lichtervelde, M., Černý, P., 2012. Granitic pegmatites as sources of strategic metals. Elements 8 (4), 275–280.
Mariet, A.L., Bégeot, C., Gimbert, F., Gauthier, J., Fluck, P., Walter-Simonnet, A.V., 2016. Past mining activities in the Vosges Mountains (eastern France): impact on vegetation and metal contamination over the past millennium. The Holocene 26 (8), 1225–1236.
Marignac, C., Cuney, M., 1999. Ore deposits of the French Massif Central: insight into the metallogenesis of the Variscan collision belt. Mineral. Deposita 34 (5), 472–504.
Markl, G., Burisch, M., Neumann, U., 2016. Natural fracking and the genesis of five-element veins. Mineral. Deposita 51 (6), 703–712.
Mazzucchelli, R., 2011. Geochemistry. In: Rutter, H. (Ed.), Field Geologists' Manual, fifth edition. Monograph Series Australasian Institute of Mining and Metallurgy, pp. 79–80.
Nédeltcheva, T., Piedallu, C., Gégout, J.C., Stussi, J.M., Boudot, J.P., Angeli, N., Dambrine, E., 2006. Influence of granite mineralogy, rainfall, vegetation and relief on stream water chemistry (Vosges Mountains, north-eastern France). Chem. Geol. 231, 1), 1–15.
Neßler, J., Seifert, T., Gutzmer, J., Müller, A., Stute, S., Kühn, K., 2013. Geology and exploration of the Li-Sn-W-Rb-Cs-deposit Zinnwald, eastern Erzgebirge, Germany. In: Proceedings of the 12th Biennial SGA Meeting. 4. pp. 1734–1737.
Norman, J.C., Haskin, L.A., 1968. The geochemistry of Sc: a comparison to the rare earth and Fe. Geochim. Cosmochim. Acta 32, 93–108.
Romer, R.L., Kroner, U., 2015. Phanerozoic tin and tungsten mineralization—tectonic controls on the distribution of enriched protoliths and heat sources for crustal melting. Gondwana Res. 31, 60–95.
Schulmann, K., Martínez Catalán, J.R., Lardeaux, J.M., Janoušek, V., Oggiano, G., 2014. The Variscan orogeny: extent, timescale and the formation of the European crust. Geol. Soc. Lond. Spec. Publ. 405, 1–6.
Shaw, D., 1968. A review of K-Rb fractionation trends by covariance analysis. Geochim. Cosmochim. Acta 32, 573–601.
Simons, B., Andersen, C.O., Shail, R.K., Jenner, F.E., 2017. Fractionation of Li, Be, Ga, Nb, Ta, In, Sn, Sb, W and Bi in the peraluminous Early Permian Variscan granites of the Cornubian Batholith: precursor processes to magmatic-hydrothermal mineralisation. Lithos 278, 491–512.
Skrzypek, E., Schulmann, K., Tabaud, A.S., Edel, J.B., 2014. Palaeozoic evolution of the Variscan Vosges Mountains. Geol. Soc. Lond. Spec. Publ. 405, 45–75.
Staude, S., Werner, W., Mordhorst, T., Wemmer, K., Jacob, D.E., Markl, G., 2012. Multi-stage Ag–Bi–Co–Ni–U and Cu–Bi vein mineralization at Wittichen, Schwarzwald, SW Germany: geological setting, ore mineralogy, and fluid evolution. Mineral. Deposita 47 (3), 251–276.
Steiner, B., 2018. Using Tellus stream sediment geochemistry to fingerprint regional geology and mineralisation systems in southeast Ireland. Irish J. Earth Sci. 36, 1–17.
Tabaud, A.-S., Whitechurch, H., Rossi, P., Schulmann, K., Guerrot, C., Cocherie, A., 2014. Devonian–Permian magmatic pulses in the northern Vosges Mountains (NE France): result of continuous subduction of the Rhenohercynian Ocean and Avalonian passive margin. Geol. Soc. Lond. Spec. Publ. 405, 197–223.
Tabaud, A.-S., Janoušek, V., Skrzypek, E., Schulmann, K., Rossi, P., Whitechurch, H., Guerrot, C., Paquette, J.-L., 2015. Chronology, petrogenesis and heat sources for successive Carboniferous magmatic events in the Southern–Central Variscan Vosges Mts (NE France). J. Geol. Soc. 172, 87–102.
Thomas, R., Tischendorf, G., 1987. Evolution of Variscan magmatic-metallogenetic processes in the Erzgebirge according to thermometric investigations. Z. Geol. Wiss. 15, 25–42.
von Eller, J.P., Pfeiffer, B., Blanalt, J.G., 1975. Carte géologique de la France à 1/50 000. 306 BRGM, Saint-Dié (46 pp.).
Walter, B.F., Burisch, M., Marks, M.A.W., Markl, G., 2017. Major element compositions of fluid inclusions from hydrothermal vein-type deposits record eroded sedimentary units in the Schwarzwald district, SW Germany. Mineral. Deposita 52 (8), 1191–1204.
Yang, X.-M., Lentz, D.R., Chi, G., Thorne, G.T., 2008. Geochemical characteristics of gold-related granitoids in southwestern New Brunswick, Canada. Lithos 104, 355–377.
Zaraisky, G.P., Korzhinskaya, V., Kotova, N., 2010. Experimental studies of Ta_2O_5 and columbite–tantalite solubility in fluoride solutions from 300 to 550 °C and 50 to 100 MPa. Mineral. Petrol. 99, 287–300.